IEEE Access
Multidisciplinary ⋮ Rapid Review ⋮ Open Access Journal

Received September 22, 2021, accepted October 5, 2021, date of publication October 15, 2021, date of current version October 25, 2021.

Digital Object Identifier 10.1109/ACCESS.2021.3120925

Sum-Rate of Cell Free Massive MIMO Systems With Power Amplifier Non-Linearity

ZAHRA MOKHTARI[1] AND RUI DINIS[2], (Senior Member, IEEE)
[1]Science and Technology Park and School of Electrical and Computer Engineering, University of Tehran, Tehran 1417935840, Iran
[2]Instituto de Telecomunicações and FCT-Nova, University of Lisbon, 1649-004 Lisbon, Portugal

Corresponding author: Zahra Mokhtari (z.mokhtari@ut.ac.ir)

This work was supported in part by the Fundação para a Ciência e Tecnologia, and in part by the Instituto de Telecomunicações under Project UIDB/50008/2020 and through the Project MASSIVE5G (POCI-01-0145-FEDER-030588 and PTDC/EEI-TEL/30588/2017) under Grant SAICT-45-2017-02.

ABSTRACT Cell free (CF) massive multiple input multiple output (mMIMO) has been suggested as a key solution to meet the high data rate demands of future wireless communications. Studying the performance of these systems in practical scenarios such as in the presence of hardware impairments is of vital importance. In this paper, we study the effect of power amplifier non-linearity on the uplink and downlink sum-rate of CF mMIMO systems. We derive closed form expressions for the uplink and downlink achievable sum-rates of orthogonal frequency division multiplexing (OFDM) based CF mMIMO systems. Our results show that in the uplink the sum-rate does not increase unlimitedly as the number of access points (AP) increases, being upper bounded, contrarily to the ideal linear case. In fact, the rate of each user is limited by the distortion signal of its power amplifier. However, in the downlink, the sum-rate of the system with non-linear power amplifiers is not bounded and increases unlimitedly with the number of APs. Our results also indicate that for the same signal to distortion ratio (SDR) at the power amplifier output or the same normalized saturation level of the power amplifiers, the relative downlink sum-rate degradation is lower than the relative uplink sum-rate degradation (both with respect to their corresponding values in the ideal linear case). In fact, our results confirm that the user side power amplifier non-linearity has higher impact on the system performance than the power amplifier non-linearity on the AP antennas.

INDEX TERMS Cell free, hardware impairment, massive MIMO, non-linearity, OFDM, power amplifier, wireless communications.

I. INTRODUCTION

Cell free (CF) massive multiple input multiple output (mMIMO) has been suggested to overcome the limitations of conventional cellular structures and to reach the data rate demands of sixth generation (6G) wireless communications [1]. In the cellular structure, the area of coverage is divided into many cells and in the center of each cell there is a base station (BS) which only serves the users in its own cell. In this structure we have inter cell interference which limits the performance of the system [2]. Also, the cell edge and cell-centric users experience different range of signal to noise ratio (SNR) in this structure [2]. However, in CF systems there is no concept of cells, and a large number of distributed antennas connected to a central processing unit (CPU), serve all the user equipments (UE) in the same time-frequency resource via time division duplex (TDD) mode operation [3], [4]. Therefore, there is no inter-cell interference in CF mMIMO systems and they have better coverage and give higher diversity gain [5]. The use of intelligent reflecting surface technology in combination of cell free massive MIMO systems has also been proposed to improve the system performance [6].

CF mMIMO, as any newly suggested technology, faces many challenges such as downlink power consumption, user localization and AP selection and hardware impairments. Some challenges and issues have been studied, however, some challenges need further investigations. In [7] the authors minimize the downlink power consumption of cell free massive MIMO systems through a Lagrange multiplier based power optimization algorithm. In [8] user localization in cell free massive MIMO systems has been studied and a dynamic two-dimensional fingerprint training scheme for user localization has been proposed. Since there is a large

The associate editor coordinating the review of this manuscript and approving it for publication was Amjad Mehmood.

number of antennas in cell free massive MIMO systems, cheaper radio frequency (RF) chains must be used to provide a cost-effective system [2], [9]. This increases the risk of the system's performance being hit by hardware impairments. Therefore, one of the important challenges in CF mMIMO systems is the system performance in presence of hardware impairments.

Most of the previous work on CF mMIMO systems have considered ideal hardware [9]–[18]. There are limited studies investigating the effect of possible hardware impairments on the CF mMIMO systems performance and further studies are required [19]–[24]. In [19] the effect of hardware impairments on energy and spectral efficiency of CF mMIMO systems has been studied. The authors in [20] analyzed the effect of transmitter and receiver hardware impairments on performance of CF mMIMO systems with low complexity receiver cooperation between APs. In both mentioned papers, the exact effect of each hardware impairment such as carrier frequency offset (CFO), power amplifier distortion (PAD) or phase noise was not considered and the hardware impairment is simply modeled by an additive distortion. The authors in [21] derived closed form expressions for uplink sum-rate of CF mMIMO systems hit by CFO. The results show that the sum-rate is upper bounded by the CFO even when the number of APs tends to infinity. In [22] closed form expressions for uplink spectral efficiency in presence of phase noise has been derived for CF mMIMO systems with minimum mean square error (MMSE) combining. In [23], the authors studied the impact of AP and user phase noise on spectral efficiency of CF mMIMO systems. They concluded that users' phase noise degrades the system's performance more than APs' phase noise. The effect of low resolution analog-to-digital converters (ADC) on the performance of CF mMIMO systems has been investigated in [24]. The results indicate that the sum-rate converges to an upper bound which is independent of the ADC resolution of the APs. Authors in [25] considered pilot spoofing attack and imperfect CSI to derive a lower bound for the secrecy rate of CF mMIMO systems in order to study the physical layer security of these systems with hardware impairments.

To the best of our knowledge, there is no work studying the effect of power amplifier non-linearity on the sum-rate of CF mMIMO systems. A system is affected by power amplifier non-linearity effects, when the power of the input signal to the amplifier exceeds the linear range of the power amplifier. Cheaper amplifiers usually have smaller linear ranges, so this increases the risk of power amplifier distortion. It is known that waveforms with high peak to average power ratios (PAPR) such as orthogonal frequency division multiplexing (OFDM) are more sensitive to power amplifier non-linearity [26].

In this paper we derive closed form expressions for the achievable sum-rate of CF mMIMO systems for both the downlink and the uplink in the presence of PAD. We derive the sum-rates considering OFDM waveform at both uplink and downlik to see how the performance degrades in presence of power amplifier non-linearity. The derived bounds give good insight on the impact of PAD on the systems performance. These results can help design a framework or a technique that is robust to power amplifier non-linearity or compensates the effect of PAD. Our analysis of the uplink shows that, unlike the ideal case with linear power amplifiers, the sum-rate of the users in presence of PAD does not increase unlimitedly as the number of AP increases. The derived uplink signal to interference plus noise ratio (SINR) of each user indicates that the uplink rate of each user is limited by the distortion signal of its own power amplifier. In the downlink, our analytical results show that the sum-rate of the system in the presence of PAD is not bounded and increases unlimitedly with the number of APs. It can be concluded from the results that the uplink sum-rate is more sensitive to power amplifier non-linearity. In other words, for the same signal to distortion ratio (SDR) at the amplifier output, the degradation of the uplink sum-rate with respect to the ideal case with no PAD, is higher than the degradation of the downlink sum-rate with respect to its ideal case with no PAD. In fact the effect of PAD in the user side on the system performance is higher than the PAD in the AP side. This is interesting, since the users usually have higher power constraint and on the other hand we can have a better amplifier at the user side and many low cost amplifiers in the multiple APs which is conceptually different from fourth generation (4G) cellular systems.

The rest of the paper is organized as follows. Section II describes the system model and Section III explains the general behaviour of a practical power amplifier and presents an appropriate model of the transmitted signals when a non-linear power amplifier is considered in our system model. In Section IV the closed form expressions for the uplink and downlink achievable sum-rates of the system in presence of PAD are derived. Section V studies the system performance through simulation results and Section VI concludes the paper.

II. SYSTEM MODEL

We consider a CF system that has L APs, where each AP is equipped with M antennas. The APs are connected to a CPU and serve K single antenna users that use simultaneously the same time and frequency resources. The channel between each user and each AP antenna is a multi-path channel with I paths. We assume the paths are independent. Coefficient $h^{(l)}_{m,k,i}$ is a zero-mean complex Gaussian variable with variance $\sigma^2_{k,i,l}$ and denotes the i-th path of the channel between the k-th user and the m-th antenna of AP l. Thus, the frequency domain channel coefficient for subcarrier n is defined as

$$H^{(l)}_{m,k,n} = \sum_{i=0}^{I-1} h^{(l)}_{m,k,i} e^{-\frac{j2\pi ni}{N}}, \tag{1}$$

where, N is the data block length. The frequency domain channel coefficients are distributed as zero mean complex Gaussian with variance of $\beta_{k,l} = \sum_{i=0}^{I-1} \sigma^2_{k,i,l}$. It is assumed that the channel coefficients of different APs and users are

independent. However, the channel coefficients of an AP antennas are correlated. In other words we have

$$E[H^{(l)}_{m,k,n}H^{(l'*)}_{m',k',n}] = C_{m,m'}\beta_{k,l}\delta(k-k')\delta(l-l'), \quad (2)$$

where, $C_{m,m'}$ is the correlation between $H^{(l)}_{m,k,n}$ and $H^{(l)}_{m',k,n}$ normalized by $\beta_{k,l}$ and $\delta(.)$ is the Dirac delta function. Therefore, we have $C_{m,m'} = 1$ for $m = m'$ and $0 \leq C_{m,m'} < 1$ for $m \neq m'$.

Since in TDD mode, due to channel reciprocity, the channel estimated in the uplink can be used in the downlink processing, we have assumed three phases in the coherence time of the channel (τ_c). The first phase is the training signal transmission for channel estimation in the uplink which has a duration of τ_{est}, and the second and third phases are the uplink and downlink data transmissions with durations τ_{ul} and τ_{dl}, respectively. Since the training sequences or pilots for channel estimation can be designed in a way that the resulting transmitted training/pilot signals have low PAPR [27]–[29], allowing the amplifiers to work in the linear region of the power amplifiers, we assume accurate channel estimation at the APs, without PAD effects. In fact, we consider a framework where each AP has full knowledge of the channel between its antennas and each user, while the CPU and the users only know the statistics of the effective channel, to reduce the feedback overheads. Fig. 1 shows the structure of a typical CF mMIMO system. In the rest of the paper, bold letters are used to present vectors and matrices.

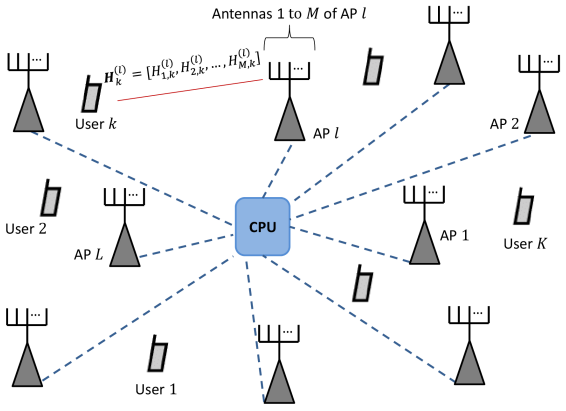

FIGURE 1. Architecture of a typical CF mMIMO system.

A. UPLINK TRANSMISSION

The n-th sample of k-th user uplink data block in frequency domain is denoted by $X^{\text{ul}}_{k,n}$. The data samples are assumed to be independent and identically distributed random variables with zero mean and variance P. Each user passes its data through an N-point inverse fast Fourier transform (IFFT) block. Therefore, the q-th time domain sample of the k-th user signal is given by

$$y^{\text{ul}}_{k,q} = \frac{1}{N}\sum_{n=0}^{N-1} X^{\text{ul}}_{k,n} e^{\frac{j2\pi nq}{N}}. \quad (3)$$

Next, cyclic prefix (CP) is added and the signal is sent to the APs.

At the receiver side, after removing the CP and passing the received data of each antenna through a fast Fourier transform (FFT) block, the received signal of the n-th subcarrier at m-th antenna of AP l is given by

$$Y^{\text{ul}(l)}_{m,n} = \sum_{k=1}^{K} H^{(l)}_{m,k,n} X^{\text{ul}}_{k,n} + N^{(l)}_{m,n}, \quad (4)$$

where $N^{(l)}_{m,n}$ is the zero-mean complex white Gaussian noise with variance σ^2 at m-th antenna of AP l. At each AP the data of the n-th subcarrier of each user is separated and equalized in the frequency domain using the $K \times M$ detection matrix $\boldsymbol{V}^{(l)}_n$. Therefore, we have

$$\hat{X}^{\text{ul}(l)}_{u,n} = \sum_{m=1}^{M}\sum_{k=1}^{K} v^{(l)}_{u,m,n} H^{(l)}_{m,k,n} X^{\text{ul}}_{k,n} + \sum_{m=1}^{M} v^{(l)}_{u,m,n} N^{(l)}_{m,n}. \quad (5)$$

where, $\hat{X}^{\text{ul}(l)}_{u,n}$ is the n-th subcarrier uplink data of user u estimated at access point l and $v^{(l)}_{u,m,n}$ is the element of row u and column m of detection matrix $\boldsymbol{V}^{(l)}_n$. Next, the APs send their estimated data and the statistics of their effective channel to the CPU. The CPU makes the final estimation as

$$\hat{X}^{\text{ul}}_{u,n} = \sum_{l=1}^{L} \hat{X}^{\text{ul}(l)}_{u,n}, \quad (6)$$

where, $\hat{X}^{\text{ul}}_{u,n}$ is the n-th subcarrier uplink data of user u estimated at the CPU.

B. DOWNLINK TRANSMISSION

In the downlink the CPU sends the data that has to be sent to each user, to the APs. At each AP and for each subcarrier, the data of the users are precoded to direct the signal of each user to that specific user. In other words, at AP l, the n-th subcarrier data of the users are precoded with an $M \times K$ precoding matrix $\boldsymbol{W}^{(l)}_n$. Therefore, the n-th subcarrier signal of antenna m at AP l can be written as

$$Y^{\text{dl}(l)}_{m,n} = \sum_{k=1}^{K} w^{(l)}_{m,k,n} X^{\text{dl}}_{k,n}, \quad (7)$$

where $w^{(l)}_{m,k,n}$ is the m-th row and k-th column of precoding matrix $\boldsymbol{W}^{(l)}_n$ and $X^{\text{dl}}_{k,n}$ is the n-th subcarrier downlink data of user k. The downlink data samples are also assumed to be independent and identically distributed random variables with zero mean and variance P. Next, the data of each antenna is passed through an N-point IFFT block. Therefore, the q-th time domain sample of signal of m-th antenna at AP l is as

$$y^{\text{dl}}_{m,q} = \frac{1}{N}\sum_{n=0}^{N-1}\sum_{k=1}^{K} w^{(l)}_{m,k,n} X^{\text{dl}}_{k,n} e^{\frac{j2\pi nq}{N}}. \quad (8)$$

At the user side, the received signal is passed through an N-point FFT block and, therefore, the received signal at subcarrier n of user u is

$$\hat{X}_{u,n}^{\mathrm{dl}} = \sum_{l=1}^{L} \sum_{m=1}^{M} H_{m,u,n}^{(l)} \sum_{k=1}^{K} w_{m,k,n}^{(l)} X_{k,n}^{\mathrm{dl}} + N_{u,n}, \qquad (9)$$

where, $N_{u,n}$ is the zero-mean complex white Gaussian noise with variance σ^2 at user u.

III. POWER AMPLIFIER NON-LINEARITY EFFECT

In the previous section an ideal linear transmitter was assumed. However, in practical systems since OFDM has high PAPR and the power amplifiers have limited linear region, the system is effected by power amplifier non-linearity. In the following two subsections we study the general behaviour of a practical power amplifier and present a suitable model of the transmitted signals when a nonlinear power amplifier is considered in our system model.

A. GENERAL BEHAVIOUR OF A PRACTICAL POWER AMPLIFIER

Fig. 2 shows the general characteristics and behaviour of a power amplifier, regarding its input and output signal power. As it is clear from this figure, a practical power amplifier has 3 working regions [30]. The first region which is the ideal region is the linear region. In this region the input signal is not corrupted at the output of the power amplifier and only its amplitude is amplified by a scalar factor. The second region is the non-linear region. In this region the input is corrupted at the power amplifier output by the non-linear effects. Finally, in the third region which is the saturated region, the input signal is highly corrupted and the output signal power is P_{sat}, no matter the input signal power level. We should note that the power amplifier has a non-linear behaviour in this region, too. There are two input power points, usually named P_{1dB} and P_s, that determine the region boundaries. Point P_{1dB} is the input power level where the actual output power is 1dB lower than what it had to be in an ideal linear power amplifier case. We should note that usually a compression point of 1dB compression is used to define the linear region. Point P_s is the smallest input power level where the output power will be saturated and no longer increase as the input power increases. For cheaper power amplifiers, the P_{1dB} is small and consequently the linear region is small and the signal is highly likely to be effected by the non-linearity.

There are different mathematical models used for modeling the behaviour of practical power amplifiers. One of the most used model in cellular communications is the *Rapp model*. In the *Rapp model* the relation between the input signal of the power amplifier and the output is as [31]

$$y_{\mathrm{out}} = \frac{x_{\mathrm{in}}}{\sqrt[2p]{1 + \left(\frac{|x_{\mathrm{in}}|}{A_{\mathrm{sat}}}\right)^{2p}}}, \qquad (10)$$

where, y_{out} is the output signal, x_{in} is the input signal, $A_{\mathrm{sat}} = \sqrt{P_{\mathrm{sat}}}$ is the saturation level and p indicates the smoothness

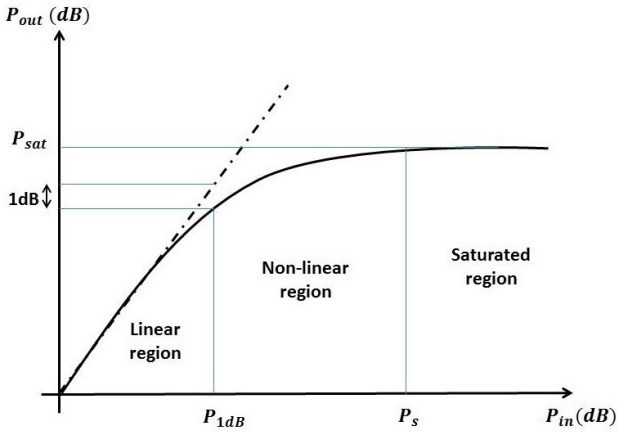

FIGURE 2. Typical output power versus input power behaviour of practical power amplifiers.

of transferring from linear region to saturated region. When we have a practical power amplifier and the input signal has high PAPR, the parts of the signal with higher input power are clipped in time domain and therefore we have out-of-band radiation in frequency domain [32]. Fig. 3 shows the power spectrum of the output signal of *Rapp model* with $p = 2$ for different normalized saturation levels $A_{n_{\mathrm{sat}}} = \frac{A_{\mathrm{sat}}}{\sqrt{P_{\mathrm{in}}}}$. As it is clear from this figure, as the normalized saturation level decreases the effect of non-linearity and consequently out-of-band radiation increases. We should note that the analysis in this paper apply to any bandpass memoryless non-linear power amplifier model and we have considered the *Rapp model* as an example.

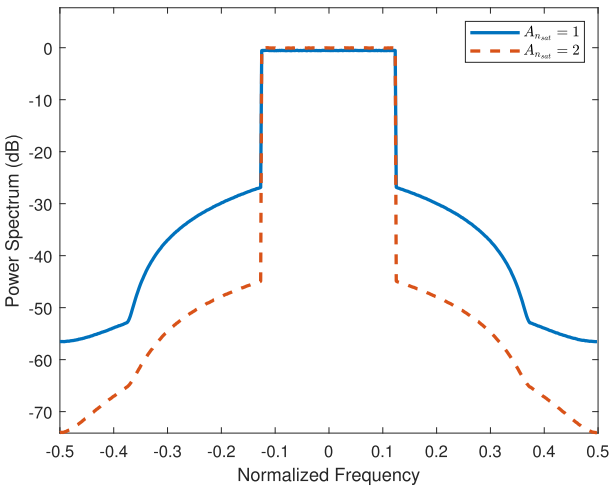

FIGURE 3. Out of band radiation analysis for *Rapp model* with $p = 2$ and different normalized saturation levels.

B. SIGNAL MODEL IN PRESENCE OF POWER AMPLIFIER NON-LINEARITY

In this subsection we will discuss how the power amplifier non-linearity will effect signals in our system model by using an appropriate model with the aid of *Bussgang Theorem* [33].

According to this theorem, if the input signal (x_{in}) of a memoryless non-linear function is Gaussian, the output of the function can be written as a scaled version of the input signal plus a distortion term, which is uncorrelated with the input signal. Therefore, we have

$$y_{\text{out}} = \alpha x_{\text{in}} + \eta_{\text{dis}}, \tag{11}$$

where α is the scalar factor and is equal to the correlation between the input and output signal ($\alpha = E[y_{\text{out}} x_{\text{in}}^*]/E[|x_{\text{in}}|^2]$) and η_{dis} is the distortion signal with zero mean and variance σ_{dis}^2. We should note that $\sigma_{\text{dis}}^2 = P_{\text{out}} - \alpha^2 P_{\text{in}}$, where P_{out} and P_{in} are the output and input signal power of the amplifier, respectively. Although the distortion is not Gaussian in the time domain and its distribution is a function of the normalized saturation level and the type of non-linear distortion, in the frequency domain the distortion is approximately Gaussian [34], [35]. It has been shown that this model properly fits the non-linear effects of the system on Gaussian input signals [36]. In the following we will discuss how the behaviour of the power amplifier in the three different regions can be interpreted with this model. In the ideal linear region, since the output signal is only the amplified version of the input signal, α is the amplification factor which without loss of generality we have assumed 1 in our system model, and the power of the distortion signal is $\sigma_{\text{dis}}^2 = 0$. In the non-linear and saturated regions we have both terms in the right hand side of equation (11). As the input power increases in these regions, α decreases and the power of the distortion signal increases. Fig. 4 shows the output signal power, α and distortion signal power versus input signal power for the *Rapp model* with $A_{\text{sat}} = 1$ and $p = 2$ and an OFDM input signals (which is approximately zero mean complex Gaussian). This figure also confirms the fact that as the input power and the non-linearity effect increase, α decreases with respect to 1 and the power of the distortion signal increases.

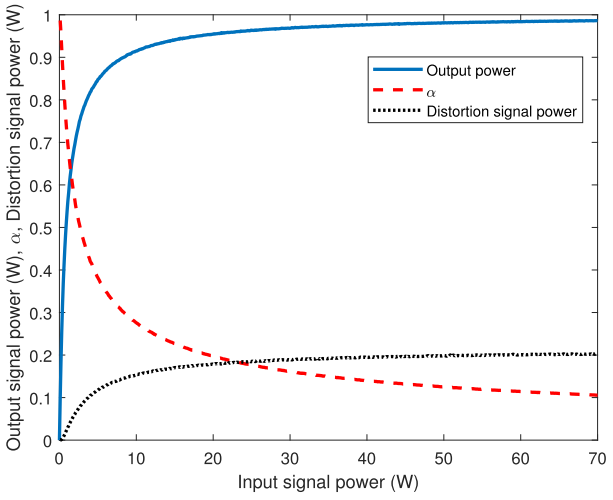

FIGURE 4. Output signal power, α and distortion signal power versus input signal power for the *Rapp model* with $A_{\text{sat}} = 1$ and $p = 2$.

Fig. 5 shows the SDR versus the normalized saturation level for the *Rapp model* with $A_{\text{sat}} = 1$ and $p = 2$ and an OFDM input signal. We should note that the signal to distortion ratio is defined as

$$\text{SDR} = \frac{|\alpha|^2 P_{\text{in}}}{\sigma_{\text{dis}}^2}$$

As expected the SDR increases as the normalized saturation level increases.

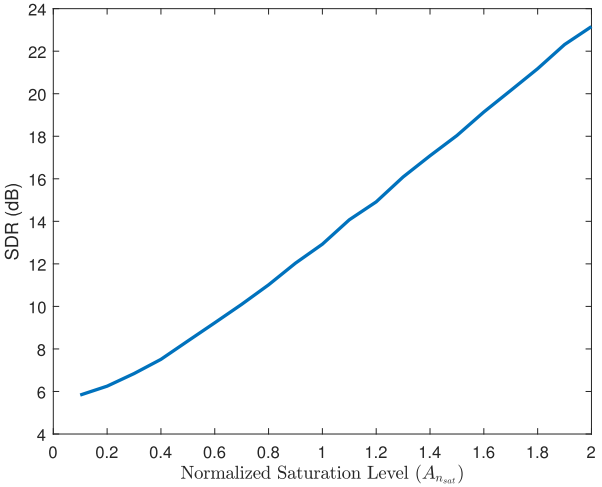

FIGURE 5. SDR versus the normalized saturation level for the *Rapp model* with $A_{\text{sat}} = 1$ and $p = 2$.

By using the central limit theorem in our system model, it can be shown that $y_{k,q}^{\text{ul}}$ in (3) and $y_{m,q}^{\text{dl}}$ in (8) are approximately Gaussian [37]. We should note that $y_{k,q}^{\text{ul}}$ and $y_{m,q}^{\text{dl}}$ are the input signals of the k-th user power amplifier in the uplink and m-th antenna of AP l power amplifier in the downlink, respectively. Therefore, we can use the *Bussgang Theorem* to model the output signal of the amplifiers in the uplink and the downlink as

$$\tilde{y}_{k,q}^{\text{ul}} = \frac{\alpha_k}{N} \sum_{n=0}^{N-1} X_{k,n}^{\text{ul}} e^{\frac{j2\pi nq}{N}} + \eta_{k,q}^{\text{ap}}, \tag{12}$$

and

$$\tilde{y}_{m,q}^{\text{dl}} = \frac{\alpha_{m,l}}{N} \sum_{n=0}^{N-1} \sum_{k=1}^{K} w_{m,k,n}^{(l)} X_{k,n}^{\text{dl}} e^{\frac{j2\pi nq}{N}} + \eta_{m,q}^{\text{ap}(l)}, \tag{13}$$

respectively. In (12), α_k is the scalar factor of power amplifier of user k and $\eta_{k,q}^{\text{ap}}$ is the distortion signal with zero mean and variance $\sigma_k^{2(\text{ap})}$, which is uncorrelated with the input signal. In (13), $\alpha_{m,l}$ is the scalar factor of power amplifier of antenna m at AP l and $\eta_{m,q}^{\text{ap}(l)}$ is the distortion signal with zero mean and variance $\sigma_{m,l}^{2(\text{ap})}$, uncorrelated with the input signal. For simplicity, and without loss of generality, we assume that the antennas at an AP use the same type of amplifiers and therefore their scalar factor and distortion signal variance is the same (the generalization to other cases is straightforward). Thus, in the rest of the paper we drop the m index in $\alpha_{m,l}$

and $\sigma^{2(\mathrm{ap})}_{m,l}$. Considering the presented non-linear model, the estimated signal at AP l in the uplink will change from (5) to

$$\hat{X}^{\mathrm{ul}(l)}_{u,n} = \sum_{m=1}^{M}\sum_{k=1}^{K} v^{(l)}_{u,m,n} H^{(l)}_{m,k,n}\left(\alpha_k X^{\mathrm{ul}}_{k,n} + N^{\mathrm{ap}}_{k,n}\right) + \sum_{m=1}^{M} v^{(l)}_{u,m,n} N^{(l)}_{m,n}. \quad (14)$$

where, $N^{\mathrm{ap}}_{k,n}$ is the distortion signal of k-th user power amplifier at subcarrier n. And the estimated signal at user u in the downlink will change from (9) to

$$\hat{X}^{\mathrm{dl}}_{u,n} = \sum_{l=1}^{L}\sum_{m=1}^{M} H^{(l)}_{m,u,n}\left(\alpha_l \sum_{k=1}^{K} w^{(l)}_{m,k,n} X^{\mathrm{dl}}_{k,n} + N^{\mathrm{ap}(l)}_{m,n}\right) + N_{u,n}, \quad (15)$$

where, $N^{\mathrm{ap}(l)}_{m,n}$ is the distortion signal of m-th antenna of AP l power amplifier at subcarrier n.

IV. ACHIEVABLE SUM-RATE

To have an insight on the effect of power amplifier non-linearity on the performance of CF mMIMO systems, in this section we derive closed form expressions for the uplink and downlink achievable sum-rates of CF mMIMO system in the presence of power amplifier distortion.

A. UPLINK SUM-RATE

To derive the closed form expression for uplink sum-rate, we assume matched filter (MF) detection matrix. Therefore, we have

$$v^{(l)}_{u,m,n} = H^{(l)*}_{m,u,n}, \quad (16)$$

for $m = 1,\ldots,M$, $k = 1,\ldots,K$, $l = 1,\ldots,L$ and $n = 0,\ldots,N-1$, where, $H^{(l)*}_{m,u,n}$ is the complex conjugate of channel coefficient $H^{(l)}_{m,u,n}$.

Since the CPU only knows the effective channel statistics, considering (16) and (14), (6) can be rewritten as

$$\hat{X}^{\mathrm{ul}}_{u,n} = \underbrace{\sum_{l=1}^{L}\sum_{m=1}^{M} \alpha_u E[|H_{m,u,n}|^2] X^{\mathrm{ul}}_{u,n}}_{\text{Desired signal}} + \Xi^{\mathrm{ul}}_{u,n}, \quad (17)$$

where, $E[.]$ is the expectation function and $\Xi^{\mathrm{ul}}_{u,n}$ is the uplink effective additive noise, defined as

$$\begin{aligned}\Xi^{\mathrm{ul}}_{u,n} &= \sum_{l=1}^{L}\sum_{m=1}^{M} \alpha_u\left(|H^{(l)}_{m,u,n}|^2 - E[|H^{(l)}_{m,u,n}|^2]\right) X^{\mathrm{ul}}_{u,n} \\ &+ \sum_{l=1}^{L}\sum_{m=1}^{M}\sum_{\substack{k=1\\k\neq u}}^{K} \alpha_k H^{(l)*}_{m,u,n} H^{(l)}_{m,k,n} X^{\mathrm{ul}}_{k,n} \\ &+ \sum_{l=1}^{L}\sum_{m=1}^{M}\sum_{k=1}^{K} H^{(l)*}_{m,u,n} H^{(l)}_{m,k,n} N^{\mathrm{ap}}_{k,n} \\ &+ \sum_{l=1}^{L}\sum_{m=1}^{M} H^{(l)*}_{m,u,n} N^{(l)}_{m,n}. \end{aligned} \quad (18)$$

Then, at the CPU, the SINR of n-th subcarrier of u-th user is given by

$$\mathrm{SINR}^{\mathrm{ul}}_{u,n} = \frac{P\left|\sum_{l=1}^{L}\sum_{m=1}^{M} \alpha_u E[|H^{(l)}_{m,u,n}|^2]\right|^2}{P_{\Xi^{\mathrm{ul}}_{u,n}}}, \quad (19)$$

where, $P_{\Xi^{\mathrm{ul}}_{u,n}}$ is the power of the uplink effective noise, given by

$$\begin{aligned} P_{\Xi^{\mathrm{ul}}_{u,n}} &= PE\left[\left|\sum_{l=1}^{L}\sum_{m=1}^{M} \alpha_u\left(|H^{(l)}_{m,u,n}|^2 - E[|H^{(l)}_{m,u,n}|^2]\right)\right|^2\right] \\ &+ PE\left[\left|\sum_{l=1}^{L}\sum_{m=1}^{M}\sum_{\substack{k=1\\k\neq u}}^{K} \alpha_k H^{(l)*}_{m,u,n} H^{(l)}_{m,k,n}\right|^2\right] \\ &+ E\left[\left|\sum_{l=1}^{L}\sum_{m=1}^{M}\sum_{k=1}^{K} H^{(l)*}_{m,u,n} H^{(l)}_{m,k,n} N^{\mathrm{ap}}_{k,n}\right|^2\right] \\ &+ \sigma^2 E\left[\left|\sum_{l=1}^{L}\sum_{m=1}^{M} H^{(l)*}_{m,u,n}\right|^2\right]. \end{aligned} \quad (20)$$

We assume $C_{m,m'} = C$ for $m \neq m'$ in (2), then with a bit of effort the uplink SINR is simplified to (21), as shown at the bottom of the next page. We have removed the index n for $\mathrm{SINR}^{\mathrm{ul}}_{u,n}$ in (21), since the derived closed form expression for the SINR is independent of the subcarrier index n.

Since the desired signal and the effective noise are uncorrelated and the CPU knows the effective channel's statistics, the achievable sum-rate of users, using Theorem 1 in [38] and considering the channel estimation overheads inherent to a TDD mode, is obtained as

$$R^{\mathrm{ul}} = \frac{\tau_{\mathrm{ul}}}{\tau_{\mathrm{est}} + \tau_{\mathrm{ul}} + \tau_{\mathrm{dl}}} \sum_{u=1}^{K} \log_2(1 + \mathrm{SINR}^{\mathrm{ul}}_u), \quad (22)$$

where, $\mathrm{SINR}^{\mathrm{ul}}_u$ is defined in (21). It can be concluded from (21) and (22) that for the case where we have no PAD ($\alpha_k = 1$ and $\sigma^{2(\mathrm{ap})}_k = 0$ for $k = 1,\ldots,K$), the sum-rate of the users is as (23), as shown at the bottom of the next page.

By comparing (22) and (23), we can conclude that the uplink sum-rate in an ideal system with linear power amplifiers increases unlimitedly as the number of APs tends to infinity. However, for the system with PAD the sum-rate is limited to

$$R^{\mathrm{ul}}_{L\to\infty} = \frac{\tau_{\mathrm{ul}}}{\tau_{\mathrm{est}} + \tau_{\mathrm{ul}} + \tau_{\mathrm{dl}}} \sum_{u=1}^{K} \log_2\left(1 + \frac{P|\alpha_u|^2}{\sigma^{2(\mathrm{ap})}_u}\right) \quad (24)$$

as $L \to \infty$. This is due to the fact that in (21) the numerator and the second term of the denominator increase with order 2 of the number of APs (L), while the first and third term of the denominator increase with order 1. Therefore, at large Ls the numerator and the second term of the denominator get dominant and the other terms of the denominator vanish

as L tends to infinity. From (24), it can be concluded that the distortion signal at the output of the power amplifier associated to each user limits the uplink rate of that user at large number of APs.

B. DOWNLINK SUM-RATE

To derive closed form expression for the downlink sum-rate, we assume MF precoder. Therefore, we have

$$w_{m,u,n}^{(l)} = \tilde{\gamma}_l H_{m,u,n}^{(l)*}, \tag{25}$$

for $m = 1,\ldots,M$, $k = 1,\ldots,K$, $l = 1,\ldots,L$ and $n = 0,\ldots,N-1$, where, $\tilde{\gamma}_l$ is the normalizing factor of the precoder to keep the transmit power of AP l at a specific value, defined as [39]

$$\tilde{\gamma}_l = \frac{1}{\sqrt{M\sum_{k=1}^{K}\beta_{k,l}}}. \tag{26}$$

Since the users only know the effective channel statistics, by considering (25) we can rewrite (15) as

$$\hat{X}_{u,n}^{\mathrm{dl}} = \underbrace{\sum_{l=1}^{L}\sum_{m=1}^{M}\tilde{\gamma}_l\alpha_l E[|H_{m,u,n}^{(l)}|^2]X_{u,n}^{\mathrm{dl}}}_{\text{Desired signal}} + \Xi_{u,n}^{\mathrm{dl}}, \tag{27}$$

where, $\Xi_{u,n}^{\mathrm{dl}}$ is the downlink effective additive noise, defined as

$$\begin{aligned}\Xi_{u,n}^{\mathrm{dl}} &= \sum_{l=1}^{L}\sum_{m=1}^{M}\tilde{\gamma}_l\alpha_l\left(|H_{m,u,n}^{(l)}|^2 - E[|H_{m,u,n}^{(l)}|^2]\right)X_{u,n}^{\mathrm{dl}} \\ &+ \sum_{l=1}^{L}\sum_{m=1}^{M}\sum_{\substack{k=1\\k\neq u}}^{K}\tilde{\gamma}_l\alpha_l H_{m,u,n}^{(l)}H_{m,k,n}^{(l)*}X_{k,n}^{\mathrm{dl}} \\ &+ \sum_{l=1}^{L}\sum_{m=1}^{M}H_{m,u,n}^{(l)}N_{m,n}^{\mathrm{ap}(l)} + N_{u,n}.\end{aligned} \tag{28}$$

Henceforth, the SINR of user u at subcarrier n is obtained as

$$\mathrm{SINR}_{u,n}^{\mathrm{dl}} = \frac{P\left|\sum_{l=1}^{L}\sum_{m=1}^{M}\tilde{\gamma}_l\alpha_l E[|H_{m,u,n}^{(l)}|^2]\right|^2}{P_{\Xi_{u,n}^{\mathrm{dl}}}}, \tag{29}$$

where, $P_{\Xi_{u,n}^{\mathrm{dl}}}$ is the power of the downlink effective noise, defined as

$$\begin{aligned}P_{\Xi_{u,n}^{\mathrm{dl}}} &= PE\left[\left|\sum_{l=1}^{L}\sum_{m=1}^{M}\tilde{\gamma}_l\alpha_l\left(|H_{m,u,n}^{(l)}|^2 - E[|H_{m,u,n}^{(l)}|^2]\right)\right|^2\right] \\ &+ PE\left[\left|\sum_{l=1}^{L}\sum_{m=1}^{M}\sum_{\substack{k=1\\k\neq u}}^{K}\tilde{\gamma}_l\alpha_l H_{m,u,n}^{(l)}H_{m,k,n}^{(l)*}\right|^2\right] \\ &+ E\left[\left|\sum_{l=1}^{L}\sum_{m=1}^{M}H_{m,u,n}^{(l)}N_{m,l,n}^{\mathrm{ap}}\right|^2\right] + \sigma^2.\end{aligned} \tag{30}$$

As in the uplink case, we consider $C_{m,m'} = C$ for $m \neq m'$ in (2). Then the SINR in (29) can be simplified as, (31), as shown at the bottom of the next page.

For simplicity, and since the derived closed form expression for the SINR is independent of the subcarrier index n, the index n for $\mathrm{SINR}_{u,n}^{\mathrm{dl}}$ in (31) was removed. Since the desired signal and the effective noise are uncorrelated, and noting that the statistics of the effective channel are known by the users, by using Theorem 1 in [38], the achievable sum-rate of the users is given by

$$R^{\mathrm{dl}} = \frac{\tau_{\mathrm{dl}}}{\tau_{\mathrm{est}}+\tau_{\mathrm{ul}}+\tau_{\mathrm{dl}}}\sum_{u=1}^{K}\log_2(1+\mathrm{SINR}_u^{\mathrm{dl}}), \tag{32}$$

where, $\mathrm{SINR}_{u,n}^{\mathrm{dl}}$ is defined in (31). It can be concluded from (31) and (32) that for the case where we have no PAD ($\alpha_l = 1$ and $\sigma_l^{2(\mathrm{ap})} = 0$ for $l = 1,\ldots,L$), the sum-rate of the users is given by

$$R_{\mathrm{ideal}}^{\mathrm{dl}} = \frac{\tau_{\mathrm{dl}}}{\tau_{\mathrm{est}}+\tau_{\mathrm{ul}}+\tau_{\mathrm{dl}}}\times\sum_{u=1}^{K}\log_2\left(1+\frac{M\left|\sum_{l=1}^{L}\tilde{\gamma}_l\beta_{u,l}\right|^2}{(1+C^2(M-1))\sum_{l=1}^{L}\sum_{k=1}^{K}\tilde{\gamma}_l^2\beta_{u,l}\beta_{k,l}+\frac{\sigma^2}{P}}\right). \tag{33}$$

From (33), it can be concluded that in the case where the power amplifiers at the APs are linear and there is no PAD, the

$$\mathrm{SINR}_u^{\mathrm{ul}} = \frac{M|\alpha_u|^2\left|\sum_{l=1}^{L}\beta_{u,l}\right|^2}{(1+C^2(M-1))\sum_{l=1}^{L}\sum_{k=1}^{K}\left(|\alpha_k|^2+\frac{\sigma_k^{2(\mathrm{ap})}}{P}\right)\beta_{u,l}\beta_{k,l}+\frac{M\sigma_u^{2(\mathrm{ap})}}{P}\left|\sum_{l=1}^{L}\beta_{u,l}\right|^2+\frac{\sigma^2}{P}\sum_{l=1}^{L}\beta_{u,l}}. \tag{21}$$

$$R_{\mathrm{ideal}}^{\mathrm{ul}} = \frac{\tau_{\mathrm{ul}}}{\tau_{\mathrm{est}}+\tau_{\mathrm{ul}}+\tau_{\mathrm{dl}}}\sum_{u=1}^{K}\log_2\left(1+\frac{M\left|\sum_{l=1}^{L}\beta_{u,l}\right|^2}{(1+C^2(M-1))\sum_{l=1}^{L}\sum_{k=1}^{K}\beta_{u,l}\beta_{k,l}+\frac{\sigma^2}{P}\sum_{l=1}^{L}\beta_{u,l}}\right). \tag{23}$$

sum-rate of the users increases unlimitedly as the number of APs tend to infinity. It can also be concluded from (31) that, for the case where we have PAD the SINR (and, consequently, the downlink sum-rate of the users) increases unlimitedly as $L \to \infty$, unlike the uplink case.

V. PERFORMANCE RESULTS

In this section we study the effect of PAD on uplink and downlik sum-rate of CF mMIMO systems through simulations. We assume that each AP has $M = 4$ antennas and the correlation between antennas of an AP is $C = 0.1$. We have $K = 10$ users and the data block length is $N = 128$. The data variance and the noise variance are $P = 1$ and $\sigma^2 = 0.5$, respectively, unless otherwise stated. We assume a multipath channel with $I = 15$ paths and uncorrelated Rayleigh fading on the different multipath components. We consider an exponential power delay profile for the channel between each transmit and received antenna. For simplicity, we assume that the power delay profile between each AP antenna and each user is the same, except in a scalar factor that differs due to different distances of the users from an AP. Therefore, we have considered $\beta_{u,l} = \gamma_{u,l} \sum_{i=0}^{I-1} e^{-i/3}$ where, $\gamma_{u,l} = 1 - \frac{|l-u|}{L}$, unless otherwise stated. We have also assumed that the training signal transmission duration for channel estimation is 10% of the coherence time of the channel ($\tau_{\text{est}} = 0.1\tau_c$) and, to have a fair comparison, we have assumed equal uplink and downlink data transmission durations ($\tau_{\text{ul}} = \tau_{\text{dl}}$).

Fig. 6 and Fig. 7 show the uplink and downlink sum-rate of CF mMIMO systems with and without PAD versus number of APs, respectively. In these figures the scalar factor is $\alpha = 0.9$ and the distortion signal variance is $\sigma^{2(\text{ap})} = 0.1$. For simplicity, we have assumed the same scalar factor α and distortion signal variance $\sigma^{2(\text{ap})}$ for all the uplink and downlink power amplifiers in these figures. We have also assumed $\beta_{u,l} = (1 - \frac{|l-u|}{150}) \sum_{i=0}^{I-1} e^{-i/3}$ in these two figures. As it is clear form Fig. 6, the uplink sum-rate of the system with PAD, unlike the ideal case with no PAD, is bounded by the black line even when $L \to \infty$. In Fig. 7, however, the sum-rate of the system hit by PAD is not degraded much with respect to the ideal case with no PAD and does not tend to an upper bound at large Ls. It can be concluded from these two figures that increasing the number of APs in the system with PAD has higher impact on the downlink sum-rate than the uplink sum-rate. For example, if we increase the number of APs from $L = 50$ to $L = 100$ the downlink sum-rate increases for about 95% while the uplink sum-rate increases for only 17.5%.

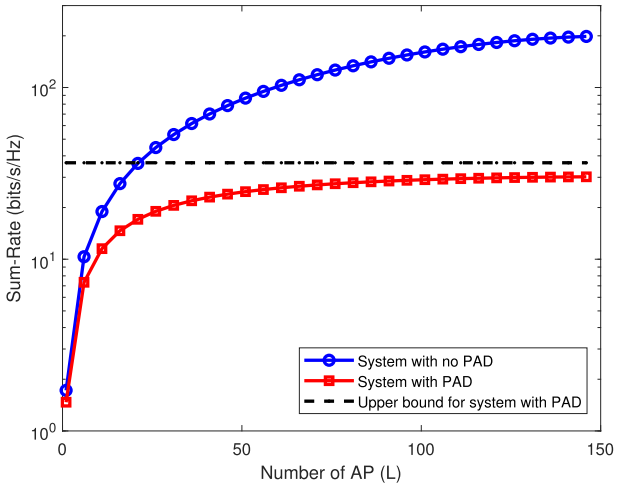

FIGURE 6. Uplink sum-rate versus L for $\alpha_k = 0.9$ and $\sigma_k^{2(\text{ap})} = 0.1$.

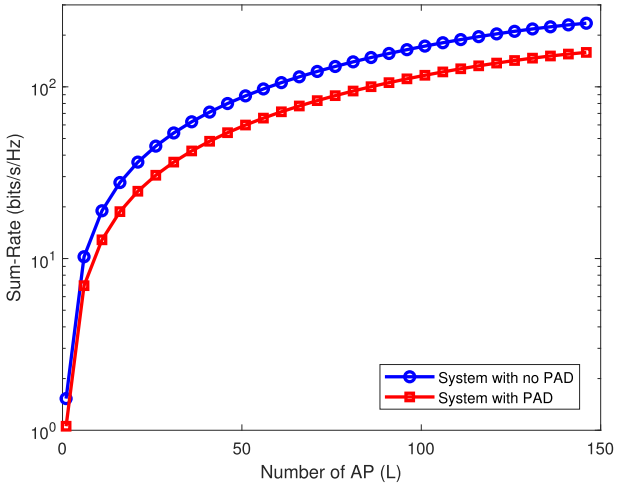

FIGURE 7. Downlink sum-rate versus L for $\alpha_l = 0.9$ and $\sigma_l^{2(\text{ap})} = 0.1$.

Fig. 8 and Fig. 9 show the uplink and downlink sum-rate of the CF mMIMO system versus SDR for $L = 100$, respectively. We have assumed no thermal noise ($\sigma^2 = 0$) in these figures, to study only the effect of power amplifier non-linearity on the sum-rates. As predicted, the uplink and downlink sum-rates of the system degrade as the signal to distortion ratio at the power amplifier output decreases and the speed of this degradation is higher at smaller SDRs. These figures also show that when SDR tends to infinity, the uplink and downlink sum-rates converge to their corresponding values in the ideal case with no PAD. It can be concluded

$$\text{SINR}_u^{\text{dl}} = \frac{M \left| \sum_{l=1}^{L} \tilde{\gamma}_l \alpha_l \beta_{u,l} \right|^2}{(1 + C^2(M-1)) \sum_{l=1}^{L} \sum_{k=1}^{K} \tilde{\gamma}_l^2 |\alpha_l|^2 \beta_{u,l} \beta_{k,l} + \frac{1}{P} \sum_{l=1}^{L} \beta_{u,l} \sigma_l^{2(\text{ap})} + \frac{\sigma^2}{P}}. \tag{31}$$

from Fig. 8 and Fig. 9 that for a specific SDR, the relative degradation of the uplink sum-rate is higher than the relative degradation of the downlink sum-rate with respect to their corresponding values in the case with no PAD. For example, for SDR= 10 dB, the uplink sum-rate degrades for about 76% compared to its value in the case with no PAD, while the downlink sum-rate only degrades 8.8% compared to the case with no PAD.

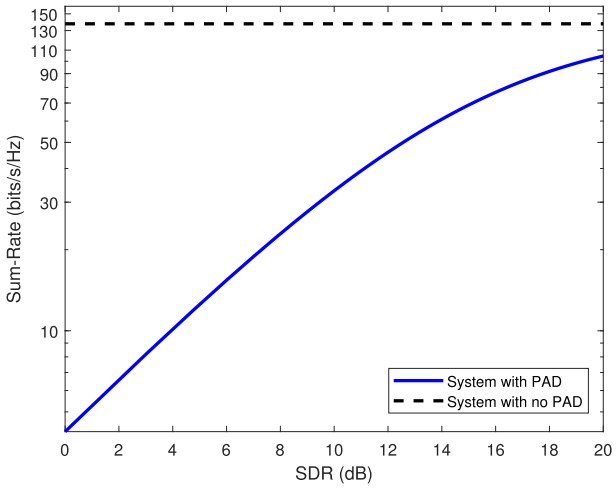

FIGURE 8. Uplink sum-rate versus SDR for $L = 100$ and $\sigma^2 = 0$.

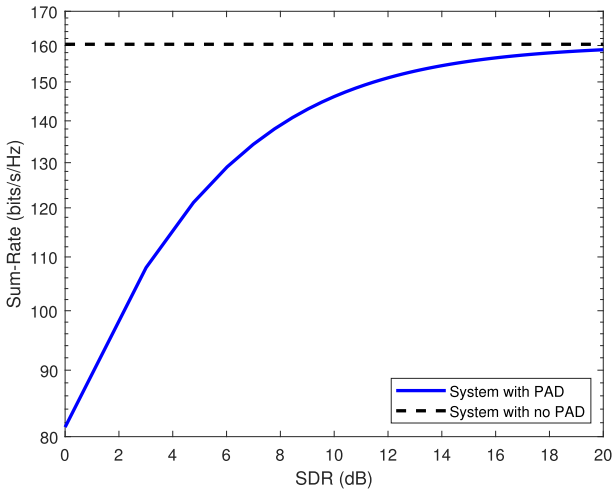

FIGURE 9. Downlink sum-rate versus SDR for $L = 100$ and $\sigma^2 = 0$.

Fig. 10 and Fig. 11 show the uplink and downlink sum-rates versus normalized saturation level of the *Rapp model* with $p = 2$, respectively. We have $L = 100$ access points in these figures. These figures indicate that, as the normalized saturation level decreases and consequently the non-linearity effect increases, the uplink and downlink sum-rates decrease. These figures also confirm the fact that the uplink sum-rate is more sensitive to power amplifier non-linearity than the downlink sum-rate. For example, for normalized saturation level $A_{n_{\text{sat}}} = 1$, the uplink sum-rate degrades for about 61% compared to the uplink sum-rate value in the case with no PAD (dashed black line in Fig. 8). However, the downlink sum-rate only degrades for about 4.6%. From the analysis in this section we can conclude that the user power amplifier non-linearity has higher effect on the system performance than the AP antennas power amplifier non-linearity.

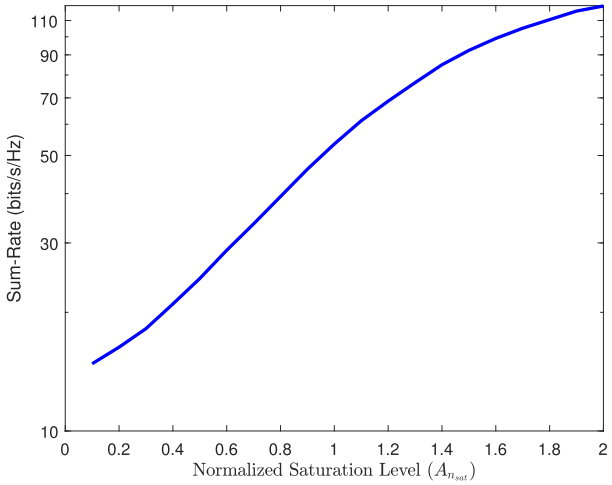

FIGURE 10. Uplink sum-rate versus normalized saturation level for $L = 100$ and $\sigma^2 = 0$.

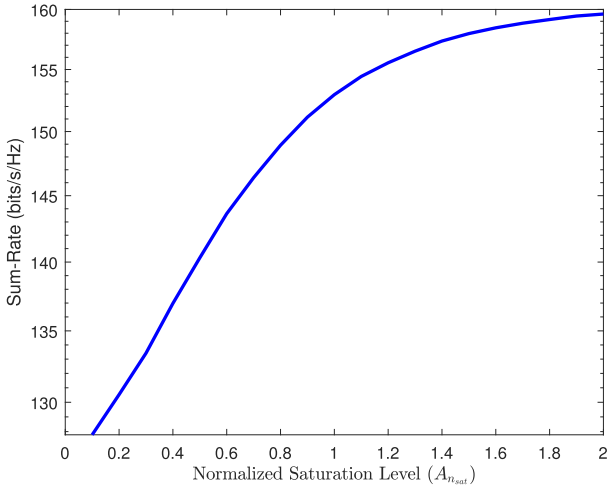

FIGURE 11. Downlink sum-rate versus normalized saturation level for $L = 100$ and $\sigma^2 = 0$.

Fig. 12 and Fig. 13 compare the uplink and downlink sum-rate of CF mMIMO system with cellular mMIMO system, respectively. In these figures we have assumed the same number of users ($K = 10$) distributed in an area and that there are two ways to serve them. In the first case the users are served by a cell free structure and in the second case they are served by a single mMIMO base station in a cellular structure. To have a fair comparison we have assumed that the total number of downlink transmit antennas and the total number of uplink receive antennas are the same in both structures. In other words in the cell free structure we have L single antenna APs and in the cellular structure we have one base station with M antennas, where $M = L$. In these two

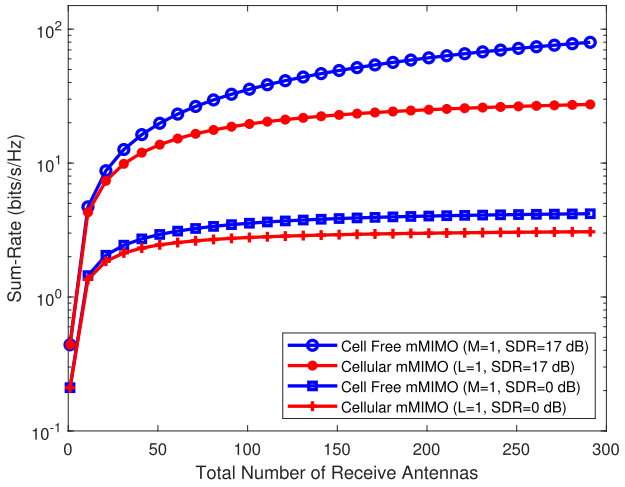

FIGURE 12. Uplink sum-rate versus total number of uplink receive antennas for different SDR values, and $\sigma^2 = 0$.

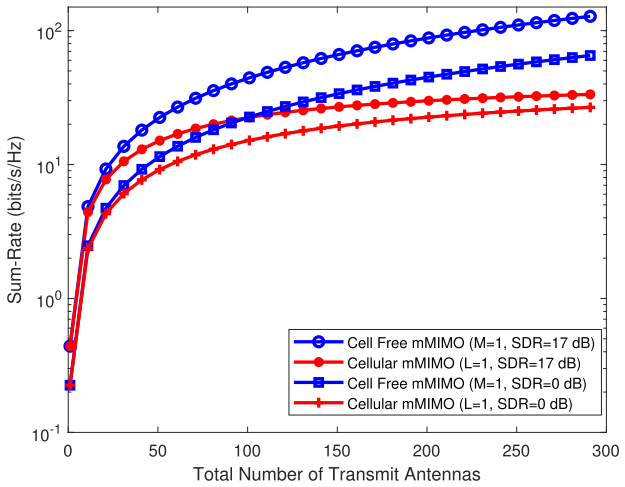

FIGURE 13. Downlink sum-rate versus total number of downlink transmit antennas for different SDR values, and $\sigma^2 = 0$.

figures we have assumed $\beta_{u,l} = (1 - \frac{|l-40u|}{400}) \sum_{i=0}^{I-1} e^{-i/3}$. Fig. 12 shows the uplink sum-rate versus total number of uplink received antennas for different SDR values for both structures. As it is clear from this figure cell free structure has higher sum-rate, specially at large number of receive antennas, due to higher diversity and better coverage. It can be concluded from the figure that the performance gap between the two structure increases as the number of total uplink receive antennas increases. It can also be concluded that the performance gap between the two structure is larger for higher SDR values (i.e., stronger nonlinear distortion effects). For example for 100 total receive antennas, the performance gap between the two structures for SDR= 0 dB and SDR= 17 dB is about 1 (bits/s/Hz) and 16 (bits/s/Hz), respectively. This is because at higher SDR the difference between the diversity gain of the two systems gets dominant. However, at small SDR values the power amplifier distortion effect is dominant.

Fig. 13 indicates the downlink sum-rate versus total number of downlink transmit antennas for different SDR values for both structures. As it is clear from this figure, the downlink sum-rate in cell free structure is also higher than the downlink sum-rate in cellular structure, specially at large number of transmit antennas, due to higher diversity and better coverage of cell free structure. It can be concluded from this that the downlink sum-rate in the cellular structure, unlike the cell free structure, is upper bounded, even with a large number of antennas [37].

VI. CONCLUSION

In this paper, we studied the effect of PAD on the uplink and downlink sum-rate of CF mMIMO systems. We derived closed form expressions for the uplink and downlink achievable sum-rates. The results showed that the uplink sum-rate is upper bounded even when the number of APs tends to infinity. However, the downlink sum-rate increases unlimitedly as number of APs grows. The limiting factor in uplink rate of each user is the power amplifier distortion signal of that user. The results also showed that the uplink sum-rate is more sensitive to power amplifier non-linearity than the downlink sum-rate. In other words, for the same SDR and normalized saturation level, the uplink sum-rate degrades significantly higher than the downlink sum-rate compared to their corresponding values in the case of ideal linear power amplifiers.

REFERENCES

[1] H. Q. Ngo, A. Ashikhmin, H. Yang, E. G. Larsson, and T. L. Marzetta, "Cell-free massive MIMO versus small cells," *IEEE Trans. Wireless Commun.*, vol. 16, no. 3, pp. 1834–1850, Mar. 2017.

[2] S. Chen, J. Zhang, J. Zhang, E. Björnson, and B. Ai, "A survey on user-centric cell-free massive MIMO systems," 2021, *arXiv:2104.13667*. [Online]. Available: http://arxiv.org/abs/2104.13667

[3] O. T. Demir, E. Björnson, and L. Sanguinetti, "Foundations of user-centric cell-free massive MIMO," *Found. Trends Signal Process.*, vol. 14, nos. 3–4, pp. 162–472, 2021.

[4] G. Interdonato, E. Björnson, H. Quoc Ngo, P. Frenger, and E. G. Larsson, "Ubiquitous cell-free massive MIMO communications," *EURASIP J. Wireless Commun. Netw.*, vol. 2019, no. 1, pp. 1–13, Dec. 2019.

[5] S.-N. Jin, D.-W. Yue, and H. H. Nguyen, "Spectral and energy efficiency in cell-free massive MIMO systems over correlated Rician fading," *IEEE Syst. J.*, vol. 15, no. 2, pp. 2822–2833, Jun. 2021.

[6] T. Zhou, K. Xu, X. Xia, W. Xie, and J. Xu, "Achievable rate optimization for aerial intelligent reflecting surface-aided cell-free massive MIMO system," *IEEE Access*, vol. 9, pp. 3828–3837, 2021.

[7] J. Qiu, K. Xu, X. Xia, Z. Shen, and W. Xie, "Downlink power optimization for cell-free massive MIMO over spatially correlated Rayleigh fading channels," *IEEE Access*, vol. 8, pp. 56214–56227, 2020.

[8] Z. Shen, K. Xu, and X. Xia, "2D fingerprinting-based localization for mmWave cell-free massive MIMO systems," *IEEE Commun. Lett.*, early access, Sep. 3, 2021, doi: 10.1109/LCOMM.2021.3109645.

[9] E. Nayebi, A. Ashikhmin, T. L. Marzetta, H. Yang, and B. D. Rao, "Precoding and power optimization in cell-free massive MIMO systems," *IEEE Trans. Wireless Commun.*, vol. 16, no. 7, pp. 4445–4459, Jul. 2017.

[10] E. Nayebi, A. Ashikhmin, T. L. Marzetta, and B. D. Rao, "Performance of cell-free massive MIMO systems with MMSE and LSFD receivers," in *Proc. 50th Asilomar Conf. Signals, Syst. Comput.*, Nov. 2016, pp. 203–207.

[11] Z. Wang, J. Zhang, E. Bjornson, and B. Ai, "Uplink performance of cell-free massive MIMO over spatially correlated rician fading channels," *IEEE Commun. Lett.*, vol. 25, no. 4, pp. 1348–1352, Apr. 2021.

[12] T. C. Mai, H. Q. Ngo, and T. Q. Duong, "Downlink spectral efficiency of cell-free massive MIMO systems with multi-antenna users," *IEEE Trans. Commun.*, vol. 68, no. 8, pp. 4803–4815, Aug. 2020.

[13] L. D. Nguyen, T. Q. Duong, H. Q. Ngo, and K. Tourki, "Energy efficiency in cell-free massive MIMO with zero-forcing precoding design," *IEEE Commun. Lett.*, vol. 21, no. 8, pp. 1871–1874, Aug. 2017.
[14] G. Interdonato, M. Karlsson, E. Bjornson, and E. G. Larsson, "Local partial zero-forcing precoding for cell-free massive MIMO," *IEEE Trans. Wireless Commun.*, vol. 19, no. 7, pp. 4758–4774, Jul. 2020.
[15] H. Q. Ngo, L.-N. Tran, T. Q. Duong, M. Matthaiou, and E. G. Larsson, "On the total energy efficiency of cell-free massive MIMO," *IEEE Trans. Green Commun. Netw.*, vol. 2, no. 1, pp. 25–39, Mar. 2017.
[16] H. Liu, J. Zhang, X. Zhang, A. Kurniawan, T. Juhana, and B. Ai, "Tabu-Search-Based pilot assignment for cell-free massive MIMO systems," *IEEE Trans. Veh. Technol.*, vol. 69, no. 2, pp. 2286–2290, Feb. 2020.
[17] M. Attarifar, A. Abbasfar, and A. Lozano, "Random vs structured pilot assignment in cell-free massive MIMO wireless networks," in *Proc. IEEE ICC Workshops*, May 2018, pp. 1–6.
[18] T. H. Nguyen, T. K. Nguyen, H. D. Han, and V. D. Nguyen, "Optimal power control and load balancing for uplink cell-free multi-user massive MIMO," *IEEE Access*, vol. 6, pp. 14462–14473, 2018.
[19] J. Zhang, X. Xue, E. Björnson, B. Ai, and S. Jin, "Performance analysis and power control of cell-free massive MIMO systems with hardware impairments," *IEEE Access*, vol. 6, pp. 55302–55314, 2018.
[20] J. Zheng, J. Zhang, L. Zhang, X. Zhang, and B. Ai, "Efficient receiver design for uplink cell-free massive MIMO with hardware impairments," *IEEE Trans. Veh. Technol.*, vol. 69, no. 4, pp. 4537–4541, Apr. 2020.
[21] Z. Mokhtari and R. Dinis, "Residual CFO effect on uplink sum-rate of cell free massive MIMO systems," in *Proc. IEEE VTC2021-Fall*, May 2021, pp. 1–5, Paper 5.
[22] A. K. Papazafeiropoulos, E. Björnson, P. Kourtessis, S. Chatzinotasy, and J. M. Senior, "Scalable cell-free massive MIMO systems with hardware impairments," *IEEE Int. Symp. Pers. Indoor Mob. Radio Commun.*, Sep. 2020, pp. 1–7.
[23] S.-N. Jin, D.-W. Yue, and H. H. Nguyen, "Spectral efficiency of a frequency-selective cell-free massive MIMO system with phase noise," *IEEE Wireless Commun. Lett.*, vol. 10, no. 3, pp. 483–487, Mar. 2021.
[24] X. Hu, C. Zhong, X. Chen, W. Xu, H. Lin, and Z. Zhang, "Cell-free massive MIMO systems with low resolution ADCs," *IEEE Trans. Commun.*, vol. 67, no. 10, pp. 6844–6857, Oct. 2019.
[25] X. Zhang, D. Guo, K. An, and B. Zhang, "Secure communications over cell-free massive MIMO networks with hardware impairments," *IEEE Syst. J.*, vol. 14, no. 2, pp. 1909–1920, Jun. 2020.
[26] J. C. Ortíz-Cornejo and J. A. Pardiñas-Mir, "OFDM system and peak to average power ratio reduction methods," *ECORFAN J.*, vol. 3, no. 5, pp. 1–9, Dec. 2017.
[27] E. Manasseh, S. Ohno, and M. Nakamoto, "Design of low PAPR preamble and pilot symbol for channel estimation in OFDM systems," *Int. J. Innov. Comput. Inf. Control*, vol. 7, no. 1, pp. 39–50, 2011.
[28] C. D. Moffatt and J. E. Hoffmann, "Low peak-to-average power ratio (PAPR) preamble for orthogonal frequency division multiplexing (OFDM) communications," U.S. Patent 0 080 309 A1, Apr. 10, 2010. [Online]. Available: https://patents.google.com/patent/US20100080309
[29] J. Oliver, R. Aravind, and K. M. M. Prabhu, "Pilot sequence design for improving OFDM channel estimation in the presence of CFO," in *Proc. SPCOM*, Bangalore, India, Jul. 2010, pp. 1–5.
[30] A. Borel, V. Barzdänas, and A. Vasjanov, "Linearization as a solution for power amplifier imperfections: A review of methods," *Electronics*, vol. 10, no. 9, p. 1073, May 2021.
[31] C. Rapp, "Effects of HPA-nonlinearity on a 4-DPSK/OFDM signal for a digital sound broadcasting system," in *proc. Eur. Conf. Netw. Commun.*, Oct. 1991, pp. 179–184.
[32] P. Albrecht and I. Cosovic, "On the out-of-band radiation reduction in OFDM systems," in *Proc. IEEE Wireless Commun. Netw. Conf.*, Mar. 2008, pp. 559–564.
[33] J. J. Bussgang, "Crosscorrelation functions of amplitude-distorted Gaussian signals," Res. Lab. Electron., Massachusetts Inst. Technol., Cambridge, MA, USA, Tech. Rep. 216, 1952.
[34] T. Araujo and R. Dinis, "On the accuracy of the Gaussian approximation for the evaluation of nonlinear effects in OFDM signals," *IEEE Trans. Commun.*, vol. 60, no. 2, pp. 346–351, Feb. 2012.
[35] T. Araújo and R. Dinis, *Analytical Evaluation of Nonlinear Distortion Effects on Multicarrier Signals*, 1st ed. Boca Raton, FL, USA: CRC Press, 2021.
[36] O. T. Demir and E. Bjornson, "The Bussgang decomposition of nonlinear systems: Basic theory and MIMO extensions," *IEEE Signal Process. Mag.*, vol. 38, no. 1, pp. 131–136, Jan. 2021.
[37] Z. Mokhtari, M. Sabbaghian, and R. Dinis, "Massive MIMO downlink based on single carrier frequency domain processing," *IEEE Trans. Commun.*, vol. 66, no. 3, pp. 1164–1175, Mar. 2018.
[38] B. Hassibi and B. M. Hochwald, "How much training is needed in multiple-antenna wireless links?" *IEEE Trans. Inf. Theory*, vol. 49, no. 4, pp. 951–963, Apr. 2003.
[39] C. Lee, C. B. Chae, T. Kim, S. Choi, and J. Leez, "Network massive MIMO for cell-boundary users: From a precoding normalization perspective," *IEEE Globecom Workshops*, Dec. 2012, pp. 233–237.

ZAHRA MOKHTARI received the B.Sc. degree from the University of Yazd, Yazd, Iran, in 2011, and the M.Sc. and Ph.D. degrees from the University of Tehran, Tehran, Iran, in 2013 and 2019, respectively, all in electrical engineering. In 2017, she was a Visiting Researcher at the Chalmers University of Technology, Gothenburg, Sweden. She is currently a Researcher at Science and Technology Park, Iran. Her research interests include wireless communications, 5G, cell free, and cellular massive MIMO.

RUI DINIS (Senior Member, IEEE) received the Ph.D. degree from the Instituto Superior Técnico (IST), Technical University of Lisbon, Portugal, in 2001, and the Habilitation degree in telecommunications from the Faculdade de Ciências e Tecnologia (FCT), Universidade Nova de Lisboa (UNL), in 2010. He was a Researcher at the Centro de Análise e Processamento de Sinal (CAPS), IST, from 1992 to 2005, and the Instituto de Sistemas e Robótica (ISR), from 2005 to 2008. From 2001 to 2008, he was a Professor at IST. In 2003, he was an Invited Professor at Carleton University, Ottawa, Canada. Since 2009, he has been a Researcher at the Instituto de Telecomunicações (IT). He is currently an Associate Professor at FCT-UNL. He has been actively involved in several national and international research projects in the broadband wireless communications area. His research interests include transmission, estimation, and detection techniques. He is a VTS Distinguished Lecturer and an Editor of IEEE TRANSACTIONS ON WIRELESS COMMUNICATIONS, IEEE TRANSACTIONS ON COMMUNICATIONS, IEEE TRANSACTIONS ON VEHICULAR TECHNOLOGY, IEEE OPEN JOURNAL OF THE COMMUNICATIONS SOCIETY, and *Physical Communication* (Elsevier). He was a guest editor for several special issues.